Am J Cancer Res 2026;16(1):28-50
www.ajcr.us /ISSN:2156-6976/ajcr0167226

Original Article

UBE2W promotes pancreatic cancer progression through regulating K63-linked ubiquitination of p53

Qiu-Ya Wei[1*], Xiao-Jun Li[2*], Tao Yong[2*], Tian-Yu Gao[2], Jian-Xing Ma[2], Dong-Yan Zhang[2], Xiang-Xiang Wei[2], Yong Fan[1], You-Cheng Zhang[1]

[1]Department of General Surgery, Lanzhou University Second Hospital, Lanzhou 730000, Gansu, China; [2]Lanzhou University, Lanzhou 730000, Gansu, China. [*]Equal contributors.

Received July 4, 2025; Accepted December 15, 2025; Epub January 15, 2026; Published January 30, 2026

Abstract: Ubiquitin-conjugating enzyme E2W (UBE2W), a member of the ubiquitin-conjugating enzyme family, is highly expressed in pancreatic cancer (PC). However, the biological function of UBE2W in cancer, particularly in human PC, remains poorly understood. This study aimed to elucidate the molecular mechanism by which UBE2W regulates the initiation and progression of PC. Integrating multiple databases and validating with clinical samples, the study identified that UBE2W is significantly overexpressed in PC tissues. High UBE2W expression is closely associated with shortened overall survival, disease-specific survival, and disease-free survival in patients. In vitro and in vivo functional experiments demonstrated that UBE2W overexpression promotes the proliferation and migration of PC cells while inhibiting apoptosis. Conversely, UBE2W knockdown significantly reduces cell viability, induces apoptosis, and suppresses tumor growth in vivo. Mechanistically, UBE2W mediates K63-linked ubiquitination of p53, regulates p53 subcellular localization, and thereby impairs p53-mediated DNA damage repair and apoptotic pathways. Collectively, UBE2W inhibits the tumor-suppressive function of p53 and promotes PC progression through the aforementioned mechanism. Targeting the UBE2W-p53 axis provides a novel therapeutic strategy for PC, and the development of related inhibitors holds promise for improving patient prognosis.

Keywords: UBE2W, p53, pancreatic cancer, K63-linked ubiquitination, DNA damage repair, apoptosis

Introduction

Pancreatic cancer (PC) is one of the most lethal malignancies in the digestive system worldwide [1]. It is highly aggressive, with early-stage disease often remaining clinically silent. Even after successful R0 surgical resection, PC patients remain prone to tumor recurrence or metastasis, resulting in a dismal 5-year survival rate of only 15%-20% [2, 3]. Unlike other cancers, PC exhibits low responsiveness to radiotherapy, chemotherapy, and immunotherapy, while research on molecular subtyping and precision therapeutic strategies remains relatively underdeveloped [4, 5]. Consequently, exploring novel approaches for PC treatment is of critical importance.

The tumor suppressor p53 plays a pivotal role in cancer prevention and is among the most crucial tumor-suppressive proteins [6, 7]. Diverse cellular stresses-including DNA damage, hyperproliferative signaling, hypoxia, oxidative stress, ribonucleotide depletion, and nutrient deprivation-activate p53, which maintains cellular homeostasis by regulating cell cycle arrest, apoptosis, and senescence [8-10]. The activation, inactivation, and degradation of p53 are primarily governed by post-translational modifications (PTMs), such as ubiquitination, acetylation, phosphorylation, methylation, neddylation, and sumoylation. Ubiquitination, a key PTM of p53, has been a major focus of research. For instance, recent studies reported that CARMIL1 promotes hepatocellular carcinoma proliferation by modulating the TRIM27/p53 axis and activating the ERK/mTOR pathway [11]. Additionally, TRIM6 facilitates cell cycle progression and growth in lung adenocarcinoma via regulation of the p53 signaling pathway [12]. These findings underscore the essential role of p53 ubiquitination in cancer development, and further elucidation of its regulatory

https://doi.org/10.62347/ZMCG3897

mechanisms may improve clinical outcomes in PC.

Ubiquitin-conjugating enzymes (E2s), a multigene family comprising over 40 known members in humans [13], execute the second step in the ubiquitination cascade and critically determine the formation of diverse ubiquitin chain types. UBE2W, a Class I E2 enzyme, consists solely of a ubiquitin-conjugating (UBC) domain. Previous studies demonstrated that UBE2W plays significant roles in DNA replication and mismatch repair regulation, with implications in malignant tumor formation and metastasis [14]. UBE2W has also been implicated in promoting endocrine therapy resistance and inducing tumor immunosuppression [15].

In this study, we identified UBE2W as highly expressed in pancreatic cancer tissues. Its overexpression promoted PC cell proliferation and migration while suppressing apoptosis, both in vitro and in vivo. Mechanistic investigations revealed that UBE2W interacts with p53 and governs its subcellular distribution. Specifically, UBE2W catalyzes the conjugation of K63-linked ubiquitin chains to lysine residues of p53, reducing its nuclear export. This ubiquitination-dependent relocalization disrupts p53-mediated DNA damage repair and apoptotic pathways, thereby accelerating PC progression. Furthermore, we developed a novel inhibitor targeting the UBE2W-p53 axis, which effectively suppresses PC advancement, offering a promising therapeutic strategy for PC patients.

Materials and methods

Data acquisition and processing

Standardized mRNA sequencing data (FPKM values) from the TCGA pan-cancer dataset (34 tumor types) and GTEx normal tissue dataset (31 normal tissue types) were acquired via the UCSC Xena platform (https://xenabrowser.net/). Key clinical variables, including overall survival (OS), disease-free survival (DFS), clinical stage (according to the 8th edition of the AJCC), and pathological grade, were simultaneously extracted.

Integration of TCGA-GTEx data was used to systematically construct a matrix comparing gene expression differences between tumor and normal tissues. Survival analyses and prognostic model development were then performed, incorporating clinical features as covariates.

mRNA profiles from 145 primary and 61 metastatic PDAC samples were obtained from the GEO database (GSE71729, GPL20769 platform). To reduce batch variation, the ComBat algorithm was used. Differential expression analysis, including clinicopathological parameters (such as T stage and lymph node metastasis), identified gene expression differences between primary and metastatic PDAC lesions.

Drug sensitivity data for PDAC samples treated with 5-fluorouracil, oxaliplatin, and paclitaxel were retrieved from the GDSC 2.0 database (https://www.cancerrxgene.org/). Sensitivity- and resistance-associated differentially expressed genes were screened by integrating these data with gene expression matrices.

The ubiquitin-conjugating enzyme (E2) gene set was downloaded from the iUUCD database (http://iuucd.biocuckoo.org).

Differential expression analysis

PDAC expression profiles were taken from TCGA and GTEx. Differential analysis between tumor and normal tissue used the R “DESeq2” package and yielded a tumor-normal DEGs1 set ($|log2FC| > 1$, $FDR < 0.05$).

Differential gene expression analysis for GSE15641 was performed using the GEO2R tool. Genes differing significantly between sample groups were identified as DEGs, using the same thresholds: $|log2FC| > 1$ and $FDR < 0.05$.

Drug sensitivity data for PDAC samples treated with 5-fluorouracil, oxaliplatin, and paclitaxel were retrieved from the GDSC database.

Sensitivity predictions for each sample were generated using the R package “pRRophetic”. IC50 values for each drug were estimated by linear regression. Samples were grouped as drug-sensitive or drug-resistant based on IC50. Differential expression analysis (e.g., “DESeq2”) then screened for gene sets (DEGs3, DEGs4, DEGs5) differing between these groups, using $|log2FC| > 1$ and $FDR < 0.05$.

Intersection analysis of the two differential expression gene sets (DEGs1, DEGs2), three drug sensitivity-related gene sets (DEGs3-5),

and one ubiquitin-conjugating enzyme gene set identified three overlapping genes: BIRC6, UBE2Q2, and UBE2W.

Pan-cancer expression and prognostic data of BIRC6, UBE2Q2, and UBE2W

Based on the TCGA pan-cancer dataset (34 tumor types), a standardized expression matrix was constructed using the R package limma. Data were transformed using the voom algorithm, and violin plots generated via ggplot2 and ggpubr were utilized to visualize differential expression of BIRC6, UBE2Q2, and UBE2W across tumor tissues and paired normal tissues.

For the prognosis of the three genes, strict quality control was applied: samples missing survival status or time were excluded; only cases with complete staging and grading were kept. This yielded 28,745 patients across 32 tumor types. Univariate Cox models using the survival package (v3.5-5) calculated hazard ratios (HRs) and 95% confidence intervals (CIs) for OS, DSS, DFS, and PFS. Prognostic significance was based on HRs, 95% CIs, and *P*-values ($P < 0.05$). Bubble plots visualized survival indices of BIRC6, UBE2Q2, and UBE2W across tumor types. Expression and prognostic accuracy were validated by the Sangerbox tool (http://www.sangerbox.com/).

Patient samples

Seventy-five pancreatic cancer tissue samples and 20 paired adjacent healthy tissues were collected at the Second Hospital of Lanzhou University (2016-2018) and stored as paraffin blocks. Sample histology was confirmed by pathologists. Pathological diagnosis and grading followed the WHO system. The study was approved by the hospital's Ethics Committee, and written informed consent was obtained from all patients. All samples were used for research.

Inclusion criteria: Patients undergoing radical resection at the Second Hospital of Lanzhou University. Pathologically confirmed pancreatic cancer diagnosis.

Exclusion criteria: Prior chemotherapy or immunotherapy. Positive surgical margins. Severe systemic comorbidities.

Clinicopathological characteristics of the patients are summarized in **Table 1**.

Cell culture and transfection

The HEK293T, Mia-Paca2, and CFPAC-1 cell lines were purchased from the American Type Culture Collection (ATCC).

These were recently authenticated by STR profiling and tested every six months for Mycoplasma; all tests were negative.

Mia-Paca2 and HEK293T cells were cultured in DMEM (Gibco, USA). CFPAC-1 cells were maintained in IMEM (Gibco, USA), both with 10% FBS (Gibco, NY, USA) at 5% CO_2, 37°C.

For gene knockdown, cells were transfected with siRNAs or infected with lentiviral shRNAs. For overexpression, cells were transfected with lentiviral particles from pLV-Flag-UBE2W, and transient transfection was used to validate the expression.

Transfection was carried out using Lipofectamine 6000 (Invitrogen) according to the manufacturer's protocol. siRNAs were at 50 nM. Plasmid transfection: 3 μg per 6-cm dish, 1 μg per well in 6-well plates.

Plasmids and antibodies

The plasmids pCMV-Flag-UBE2W, pCMV-GFP-UBE2W, pCMV-Flag-p53, pCMV-HA-p53, HA-Ub, HA-Ub-K48R, and HA-Ub-K63R were purchased from YuBio Biotechnology Co., Ltd. (Shanghai, China). Primary antibodies included the following: anti-UBE2W (PA5-67547), GFP-Tag (MA5-15256), and Cleaved Caspase-9 (PA5-105271) from Invitrogen (Chicago, USA); anti-p53 (10442-1-AP), Caspase-3 (19677-1-AP), Caspase-9 (0380-1-AP), and Cleaved Caspase-3 (25128-1-AP) from Wuhan Sanying Biotechnology Co., Ltd. (Wuhan, China); anti-Bax (A19684), Bcl-2 (A19693), p21 (A19094), γH2AX (P0687), and LAMB1 (AF3311) from ABclonal Biotechnology Co., Ltd. (Jiangsu, China); anti-HA-Tag (ab9110), Flag-Tag (ab20-5606), β-actin (ab8226), and GAPDH (ab8245) from Abcam (Cambridge, UK).

Immunohistochemistry (IHC)

Pancreatic cancer tissues and adjacent normal tissues were paraffin-embedded, baked at

Table 1. Relationships between UBE2W expression and the clinicopathological characteristics of patients with PC

Characteristic	Levels	Low expression of UBE2W	High expression of UBE2W	*P* value
Age (year)		56.69±7.29	60.00±9.09	0.114
Sex, n (%)	Female	8 (10.67%)	17 (22.67%)	0.801
	Male	18 (24.00%)	32 (42.67%)	
Tumor size (cm)		4.00±1.56	4.14±1.67	0.715
T stage, n (%)	T1+2	9 (12.00%)	21 (28.00%)	0.622
	T3+4	17 (22.67%)	28 (37.33%)	
N stage, n (%)	N0	21 (28.00%)	26 (34.67%)	0.060
	N1	4 (5.33%)	17 (22.67%)	
	N2	1 (1.30%)	6 (8.00%)	
M stage, n (%)	M0	21 (28.00%)	43 (57.33%)	0.498
	M1	5 (6.67%)	6 (8.00%)	
Differentiation status, n (%)	Poorly differentiated	5 (6.67%)	10 (13.33%)	0.984
	Moderately differentiated	17 (22.67%)	31 (41.33%)	
	Highly differentiated	4 (5.33%)	8 (10.67%)	
Vascular invasion status, n (%)	Yes	18 (24.00%)	26 (34.67%)	0.222
	No	8 (10.67%)	23 (30.67%)	
Neural tract invasion status, n (%)	Yes	14 (18.67%)	13 (17.33%)	0.024
	No	12 (16.00%)	36 (48.00%)	
Positive lymph nodes, n (%)	Yes	21 (28.00%)	27 (36.00%)	0.042
	No	5 (6.67%)	22 (29.33%)	
CA199 (U/ml), median (IQR)		252.99±294.81	450.09±381.19	0.016
CA125 (U/ml), median (IQR)		23.02±13.71	35.51±38.37	0.045
CEA (ng/ml), median (IQR)		4.79±5.85	5.26±9.83	0.799
AFP (ng/ml), median (IQR)		2.94±1.43	3.35±2.14	0.384

Note: T stage: Primary Tumor Stage; N stage: Regional Lymph Node Stage; M stage: Distant Metastasis Stage; CA199: Cancer Antigen 199; CA125: Cancer Antigen 125; CEA: Carcinoembryonic Antigen; AFP: Alpha-Fetoprotein.

65°C for 30 minutes, and then sequentially deparaffinized and rehydrated using xylene ethanol gradients, and phosphate-buffered saline (PBS) or deionized water.

For antigen retrieval, sections were heated in citrate buffer at 100°C for 20 minutes.

Endogenous peroxidase activity was blocked with 3% hydrogen peroxide for 10 minutes. Slides were blocked with 5% horse serum for 1 hour to prevent non-specific binding. Sections were incubated with anti-UBE2W primary antibody at 4°C overnight. The next day, goat anti-rabbit secondary antibody was applied for 1 hour at room temperature. Sections were stained, counterstained with hematoxylin, dehydrated through a graded ethanol series, and coverslipped.

IHC scoring

The IHC score was calculated as the product of staining intensity and percentage of positive tumor cells. Two pathologists, blinded to outcomes, independently scored the slides.

Scoring criteria

Positive Cell Proportion: 0 points (< 10%), 1 point (10-25%), 2 points (26-50%), 3 points (51-75%), 4 points (> 75%).

Staining Intensity: 0 points (no staining), 1 point (weak), 2 points (moderate), 3 points (strong).

The final IHC score ranged from 0 to 12, with scores ≤ 4 classified as low expression (-) and scores > 4 as high expression (+).

Cell proliferation, colony formation, wound healing, and transwell assays

Cell proliferation was assessed using the Cell Counting Kit-8 (CCK-8). Treated cells (1×10^3 cells/well) in 100 μL culture medium were seeded into 96-well plates (5 replicates per group) and cultured overnight. Proliferation was monitored for 1-5 days. At fixed time points daily, the medium was replaced with 100 μL fresh medium containing 10% CCK-8 reagent (10 μL CCK-8 + 90 μL medium with 10% serum). After 2 hours of incubation, absorbance at 450 nm was measured using a microplate reader. Cell growth curves were plotted using GraphPad software.

Colony formation assays were performed to evaluate proliferative capacity. Treated cells (500 cells/well) were seeded into 6-well plates (3 replicates per group) and cultured for 2 weeks. Cells were fixed with 4% formaldehyde for 30 minutes and stained with 0.1% crystal violet for 10 minutes. Visible colonies (> 50 cells per colony) were counted manually.

The migratory ability of pancreatic cancer cells was evaluated using wound healing and Transwell assays.

Treated cells were seeded into 6-well plates and cultured to 90-100% confluency. Uniform scratches (2-3 per well) were created using a sterile pipette tip. After PBS washing, serum-free medium was added, and three biological replicates were prepared for each group. Wound closure was monitored at 0, 24, 36, and 72 hours by capturing images at fixed positions under an inverted microscope.

Cell migration was assessed using 24-well Transwell chambers (Corning, NY, USA). Cells (4×10^4 in 200 μL serum-free medium) were added to the upper chamber, while the lower chamber contained medium with 10% FBS. After 48 hours of incubation, cells adhering to the lower membrane were fixed with 4% formaldehyde for 30 minutes, and non-migrated cells in the upper chamber were removed with a cotton swab. Membranes were washed with PBS, stained with 0.1% crystal violet, air-dried, and imaged.

Flow cytometric apoptosis assay

Apoptosis was detected using the Annexin V-APC/7-AAD Apoptosis Detection Kit (AP105; LIANKE Biotechnology, Hangzhou, China), which employs dual staining.

Treated cells were collected, washed with PBS, centrifuged, and resuspended in Binding Buffer. Cells were stained with Annexin V-FITC and PI in the dark for 15 minutes. Flow cytometry was performed using FL1 (Annexin V) and FL2 (PI) channels. Apoptotic populations were distinguished via scatter plots: early apoptosis (Annexin V+/PI-), late apoptosis (Annexin V+/PI+), and necrotic cells (Annexin V-/PI+). Three biological replicates were analyzed per group.

Quantitative real-time polymerase chain reaction (qRT-PCR)

Total RNA was isolated from cells using TRIzol reagent (Thermo Fisher Scientific, Shanghai, China) following the manufacturer's protocol. cDNA was synthesized using a reverse transcription kit (Agbio Biotechnology, Hunan, China). Real-time PCR amplification was performed with the SYBR Premix Ex Taq kit (Takara Biomedical Technology, Beijing, China).

Western blotting, IP, and Co-IP assays

Western blotting was performed following standard protocols.

Immunoprecipitation (IP) Procedure: After successful transfection with pCMV-Flag-UBE2W or negative control plasmids, cells were cultured for 36-48 hours. Transfected cells were harvested, lysed in IP lysis buffer, and incubated on ice for 2 hours. Lysates were centrifuged at 12,000 × g for 10 minutes at 4°C. A 60 μL aliquot of the supernatant was mixed with 5× SDS loading buffer, boiled at 100°C for 10 minutes, and saved as the input sample. The remaining supernatant was incubated with 30 μL pre-washed anti-Flag magnetic beads at 40 rpm overnight. The bead-protein complexes were immobilized using a magnet, and the supernatant was discarded. Beads were washed three times with lysis buffer. Immunoprecipitated proteins were eluted in 1× SDS loading buffer. Protein samples were loaded into gel wells and separated by electrophoresis at a constant voltage of 80 V. Gels were stained with Coomassie Brilliant Blue for 2 hours and destained with ddH2O (replaced every 30 minutes). Visible bands were excised under white light and subjected to mass spectrometry.

Co-Immunoprecipitation (Co-IP) Procedure: Cells were co-transfected with pCMV-Flag-UBE2W, pCMV-HA-p53, and negative control plasmids, followed by 36-48 hours of culture. Protein collection and preparation steps were identical to the IP protocol. Western blotting was conducted as described above.

In vivo ubiquitination assay

Cells were transfected with distinct plasmids to modulate p53 ubiquitination under specified conditions. Following transfection, 293T cells were harvested after 36-48 hours of culture and treated with MG132 (20 μM) for 8 hours to inhibit proteasomal degradation. Protein collection and sample preparation steps were identical to those described for the immunoprecipitation (IP) assay. Western blotting was performed following standard protocols.

Xenograft mouse model

Four-week-old BALB/c nude mice were purchased from Chengdu Yaokang Biotechnology Co., Ltd. The mice were randomly divided into three groups (n = 5 per group): shNC, shUBE2W-1, and shUBE2W-2. PANO2 cells (5×10^6) transduced with lentiviral vectors expressing either a negative control (LV-shNC) or UBE2W-targeting sequences (LV-shUBE2W) were subcutaneously injected into the mice to establish xenograft tumors.

Tumor size was measured every 3 days using calipers. On day 30, mice were euthanized, and tumors were completely excised for volume and weight measurement. Nude mice were anesthetized by ether inhalation and then euthanized via cervical dislocation. Tumor volume was calculated as V = 0.5 × length × width2. Excised tumors were fixed in 4% paraformaldehyde and stored for further analysis.

All experimental protocols were approved by the Animal Care and Use Committee of the Second Hospital of Lanzhou University.

Statistical analysis

Data were analyzed using Prism software (version 9.0; GraphPad Software Inc., San Diego, CA, USA). Results are expressed as mean ± SEM.

For comparisons between two groups, Student's t-test was used. For multiple groups or multiple time points, data were first analyzed by one-way analysis of variance (ANOVA) or repeated measures ANOVA (for continuous time-point data), respectively, followed by appropriate post hoc tests (e.g., Tukey's multiple comparison test) for pairwise comparisons. A P value < 0.05 was considered statistically significant.

Results

Identification of differentially expressed genes

Integrated analysis across multiple databases (TCGA, GTEx, GEO, GDSC, and iUUCD) identified two differentially expressed gene (DEG) sets: PAAD-DEG (4,919 genes) and Metastasis-DEG (3,758 genes) (**Figure 1A**, **1B**).

In addition, three DEG sets related to drug sensitivity were identified: 5-fluorouracil-DEG (747 genes), oxaliplatin-DEG (1,937 genes), and paclitaxel-DEG (758 genes) (**Figure 1C-E**).

To clarify overlaps of interest, we performed intersection analysis among the two main DEG sets, the three drug sensitivity-related gene sets, and the ubiquitin-conjugating enzyme gene set. This intersection revealed three genes common to all input sets: BIRC6, UBE2Q2, and UBE2W (**Figure 1F**).

Volcano plots were used to visualize differences in gene expression and variations in drug sensitivity (**Figure 1A-E**). A Venn diagram was used to illustrate how the gene numbers from each dataset overlap and to show the specific genes shared by all DEGs and gene sets mentioned above (**Figure 1F**).

Pan-cancer expression and prognostic significance of BIRC6, UBE2Q2, and UBE2W

Pan-cancer analysis revealed the expression patterns (**Figure 2A-C**) and prognostic outcomes (**Figure 2D-F**) of BIRC6, UBE2Q2, and UBE2W. UBE2W was notably overexpressed in pancreatic cancer and strongly correlated with poor prognosis, as shown by reduced OS, DSS, and DFI.

Pan-cancer immune correlations of UBE2W

The tumor microenvironment (TME) plays a critical role in tumor diagnosis, therapeutic

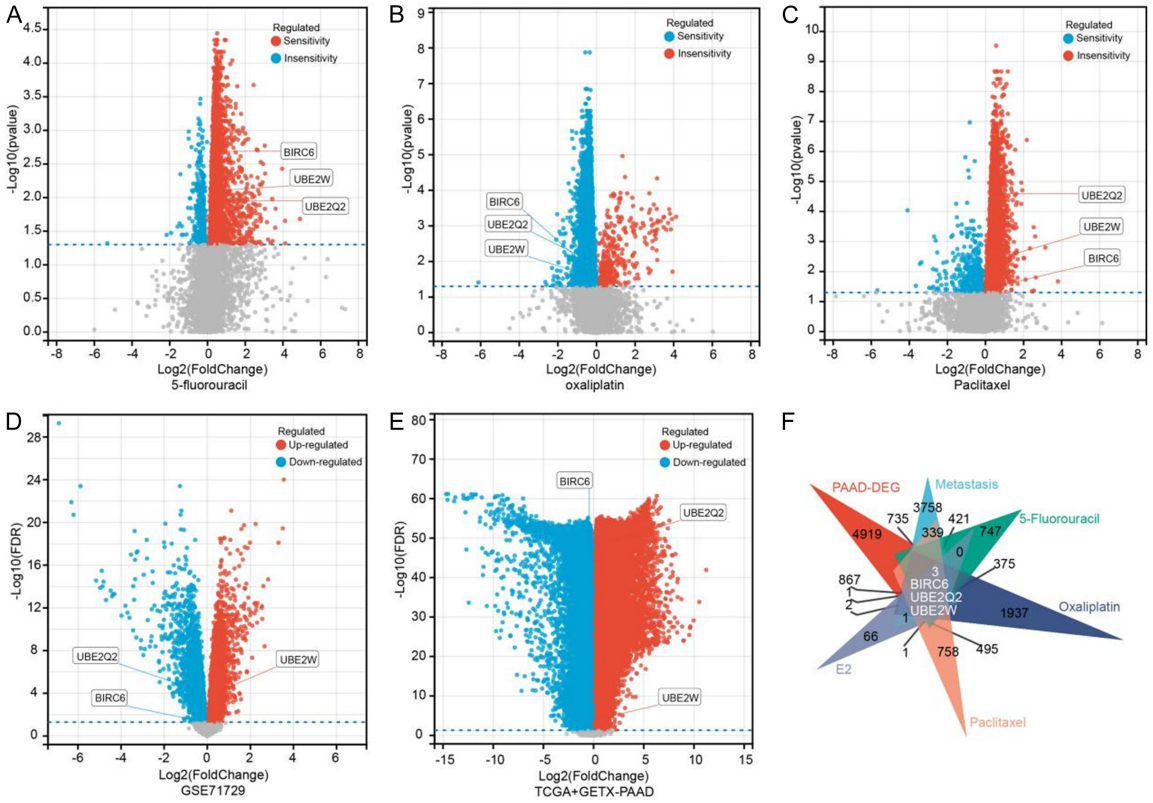

Figure 1. Acquisition of differentially expressed genes in pancreatic cancer datasets. A. Volcano plots of differentially expressed gene sets between tumor and normal tissues in pancreatic ductal adenocarcinoma datasets from TCGA and GTEx databases. B. Volcano plots of differentially expressed gene sets between in - situ and metastatic tissues in the GSE15641 pancreatic cancer dataset from the GEO database. C-E. Volcano plots of differentially expressed genes related to drug sensitivity of pancreatic ductal adenocarcinoma samples to 5-fluorouracil, oxaliplatin, and paclitaxel in the GDSC database. F. Venn diagram of the intersections of two differentially expressed gene sets, three drug - sensitivity - related differentially expressed gene sets, and one ubiquitin - conjugating enzyme gene set.

response, and prognosis. To investigate the pan-cancer relevance of UBE2W within the TME, we conducted a comprehensive analysis using the psych package in R to assess the association between UBE2W expression and immune infiltration metrics, including stromal score, immune score, and ESTIMATE score (**Figure 3A-G**). UBE2W expression showed significant correlations with immune infiltration across 16 cancer types. Eleven cancer types exhibited strong positive associations (LIHC, GBMLGG, KIRC, KIPAN, PAAD, READ, GBM, COADREAD, COAD, DLBC, LAML), whereas five showed significant negative associations (UCEC, SARC, STES, PCPG, STAD). These findings suggest that UBE2W may actively participate in remodeling the tumor-immune microenvironment.

Notably, UBE2W expression showed a significant positive association with multiple immune checkpoint-related genes, including C10orf54, CD274, HAVCR2, and IL10, across a broad range of cancer types (**Figure 3H**). Furthermore, UBE2W expression exhibited broad associations with multiple immune cell populations-including B cells, $CD4^+$ T cells, $CD8^+$ T cells, neutrophils, macrophages, and dendritic cells-across the majority of tumor types, as revealed by immune cell infiltration analysis (**Figure 3I**).

UBE2W is significantly upregulated in pancreatic cancer (PC)

We first assessed UBE2W expression in PC and normal pancreatic tissues using paraffin-embedded sections. Immunohistochemical (IHC) staining revealed markedly elevated UBE2W expression in PC tissues compared with normal controls. **Figure 4A** presents representative images of UBE2W immunostaining in

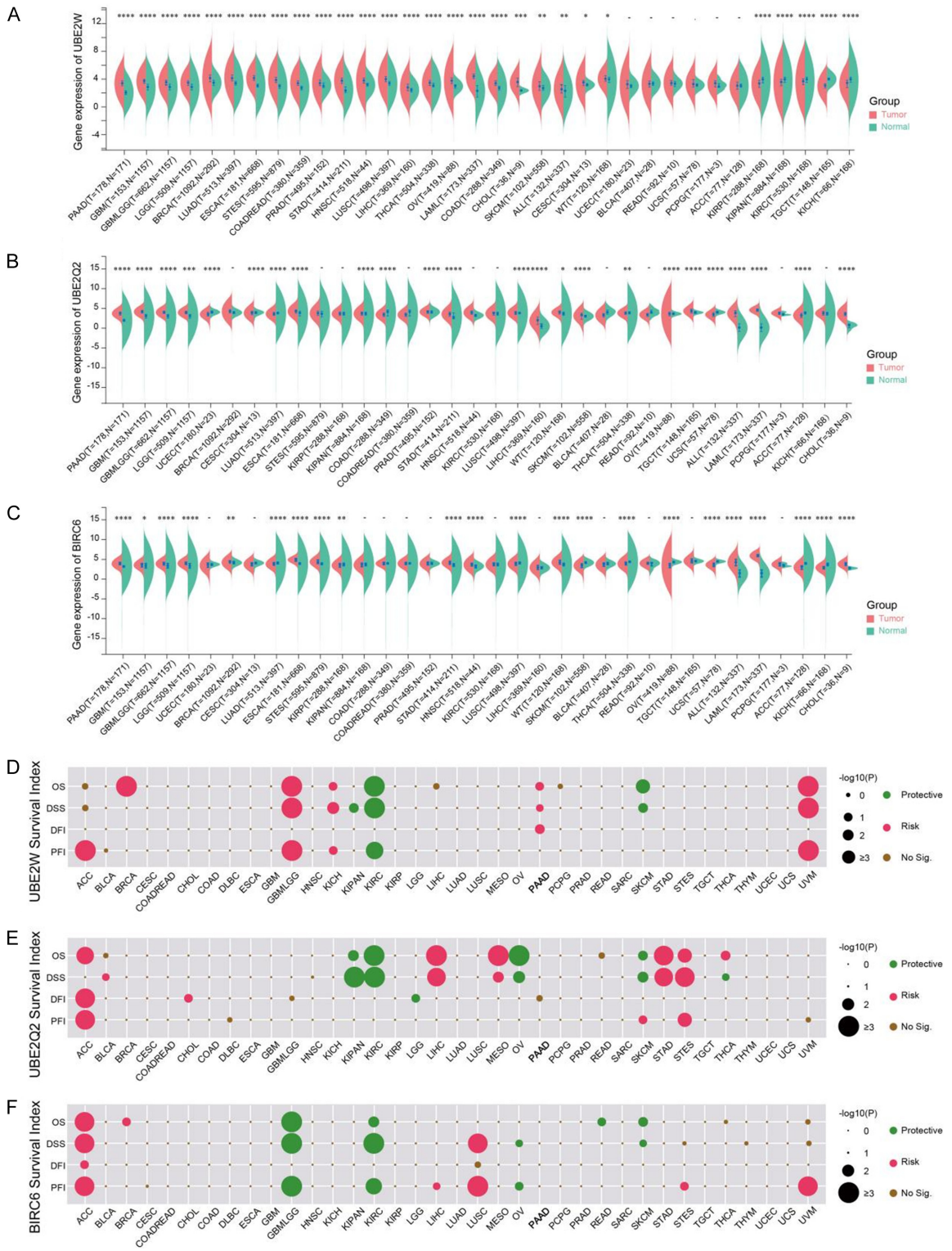

Figure 2. Expression levels and prognosis of differentially expressed genes in pan-cancer tissues. A-C. Expression of UBE2W, UBE2Q2 and BRIC6 in pan-cancer tissues; D-F. Prognosis associated with UBE2W, UBE2Q2 and BRIC6 in pan-cancer.

tumor and normal tissues at various magnifications. Furthermore, UBE2W protein levels were markedly elevated in PC cell lines compared with the normal pancreatic epithelial cell line

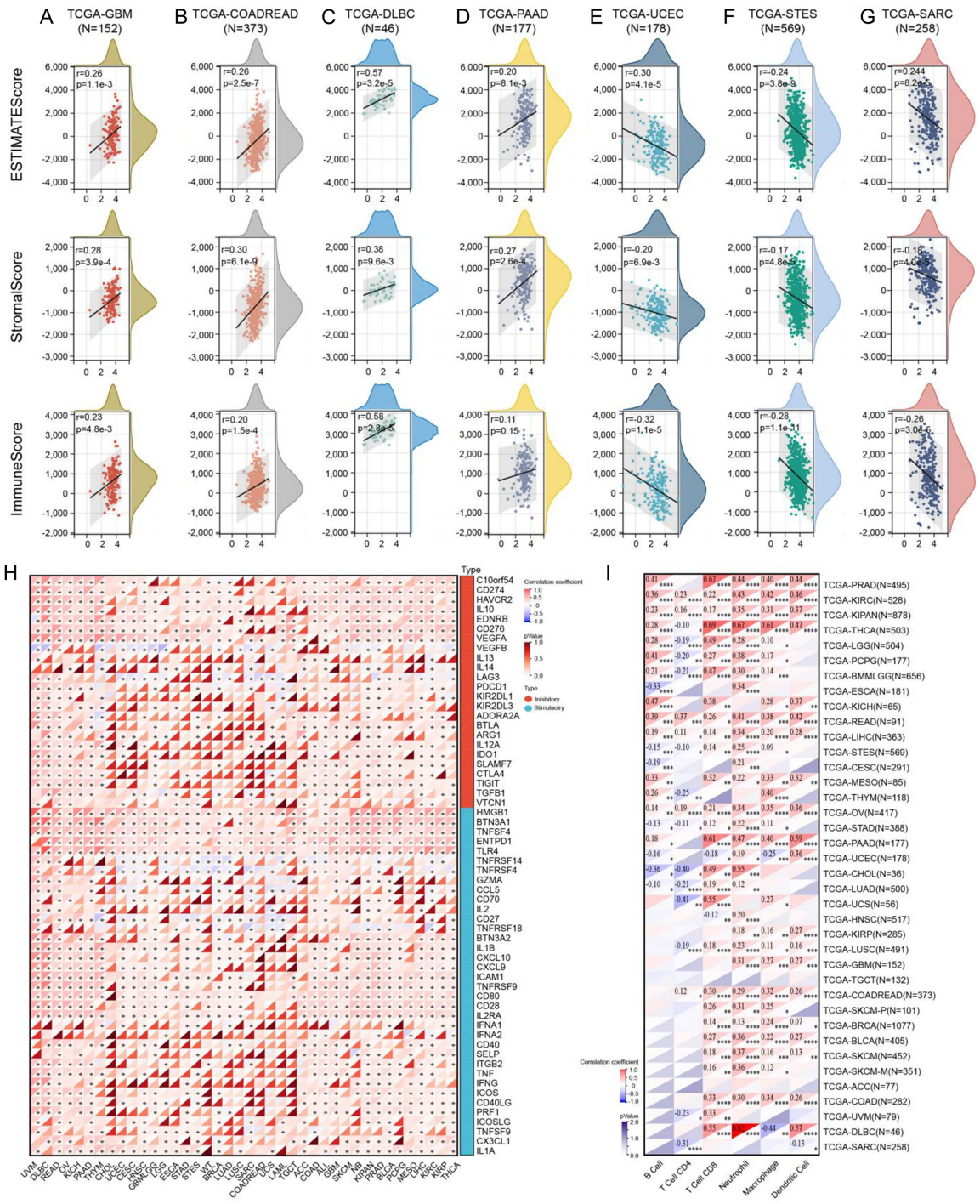

Figure 3. The correlation between UBE2W expression and immune infiltration and immune checkpoints. A-G. Correlation of UBE2W expression with StromalScore, ImmuneScore and EstimateScore in pan-cancer. H. Relationship between UBE2W and immune checkpoint genes in pan-cancer. I. Relationship between UBE2W and immune cells in pan-cancer.

hTERT-HPNE (**Figure 4B**). Quantitative real-time PCR (qRT-PCR) analysis yielded consistent results (**Figure 4C**). These findings are consistent with the elevated UBE2W expression observed in PC samples from the TCGA and GTEx datasets (**Figure 4D**).

High UBE2W expression in PC correlates with perineural invasion, lymph node metastasis, serum CA19-9, and CA125 levels

To examine the association between UBE2W expression and clinicopathological characteris-

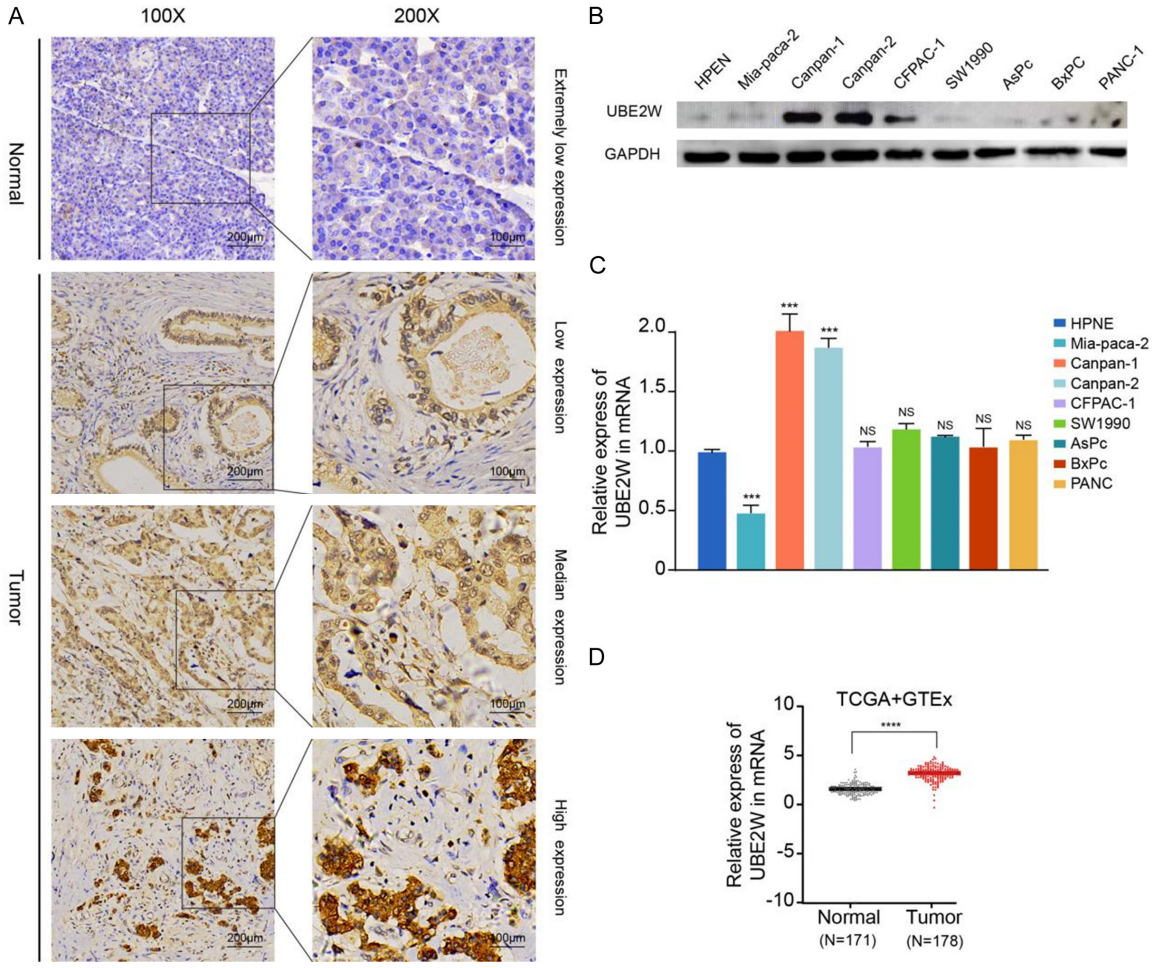

Figure 4. High expression of UBE2W in pancreatic cancer. (A) Expression of UBE2W in pancreatic cancer and normal tissues detected by immunohistochemical staining; UBE2W expression in PC cells was determined by Western blotting (B) and qRT - PCR (C); which is consistent with the expression trend in the TCGA database (D). Data are presented as the mean ± SD of at least three independent experiments. Statistical significance was determined as *P < 0.05, **P < 0.01, and ***P < 0.001.

tics, clinical data from 75 patients with PC were analyzed (**Table 1**). Patients were stratified into high- and low-expression groups according to the median UBE2W expression level determined by immunohistochemical (IHC) staining. Pearson's χ^2 test revealed significant associations between UBE2W expression and perineural invasion (P = 0.024), the number of positive lymph nodes (P = 0.042), serum carbohydrate antigen 19-9 (CA19-9) levels (P = 0.016), and serum cancer antigen 125 (CA125) levels (P = 0.045). No significant associations were identified between UBE2W expression and other clinicopathological parameters, including histological grade, age, sex, tumor size, serum alpha-fetoprotein (AFP) concentration, carcinoembryonic antigen (CEA) levels, lymphovascular invasion, or TNM stage (T, N, M). Thus, elevated UBE2W expression may represent a potential risk factor driving the initiation and progression of PC. Nevertheless, the robustness of its prognostic predictive value requires additional confirmation through comprehensive clinical studies.

High UBE2W expression is an independent prognostic risk factor in PC

To assess whether UBE2W expression functions as an independent prognostic indicator in PC, we conducted univariate and multivariate Cox proportional hazards regression analyses based on the clinicopathological variables and UBE2W expression profiles of 75 patients with

PC (**Table 2**). Univariate analysis revealed that elevated serum CA19-9 levels (HR = 1.982, 95% CI: 1.118-3.513; P = 0.049), the presence of positive lymph nodes (HR = 1.735, 95% CI: 1.138-2.643; P = 0.032), and high UBE2W expression (HR = 1.949, 95% CI: 1.253-3.028; P = 0.013) were significantly associated with poorer overall survival. In contrast, histological grade, age, sex, tumor size, serum AFP levels, CEA levels, lymphovascular invasion, perineural invasion, and TNM stage were not significantly associated with overall survival.

Variables with P < 0.05 in the univariate analysis-namely, serum CA19-9 levels, positive lymph nodes, and UBE2W expression-were incorporated into the multivariate Cox proportional hazards regression model. Multivariate analysis confirmed that high UBE2W expression (HR = 1.776, 95% CI: 1.113-2.833; P = 0.043) serves as an independent prognostic predictor of PC.

Survival follow-up data, together with IHC analysis, indicated that high UBE2W expression was associated with reduced overall survival (OS), consistent with the survival trends observed in the TCGA and GTEx datasets (**Figure 5A** and **5B**).

UBE2W promotes PC progression in vitro and in vivo

To clarify the biological function of UBE2W in PC development, we examined its effect on the proliferation of pancreatic cancer cells. We constructed UBE2W-knockdown and UBE2W-overexpressing pancreatic cancer cell lines (MIA-Paca-2 and CFPAC-1), which were successfully verified by Western blotting (**Figure 6A**, **6F**, **6O**, **6T**, **6Y**) and qRT-PCR (**Figure 6B**, **6G**, **6U**, **6Z**).

In the CCK-8 assay, knockdown of UBE2W significantly inhibited the proliferation of MIA-Paca-2 and CFPAC-1 cells (**Figure 6C** and **6H**), whereas overexpression of UBE2W markedly promoted their proliferation (**Figure 6V** and **6Aa**). Similarly, colony formation assays showed that knockdown of UBE2W substantially decreased the number of colonies formed by MIA-Paca-2 and CFPAC-1 cells (**Figure 6D**, **6E** and **6I**, **6J**), whereas UBE2W overexpression significantly increased colony formation (**Figure 6W**, **6X** and **6Ab**, **6Ac**). In the mouse tumor-bearing experiment, knockdown of UBE2W led to reduced volume and weight of tumors formed by murine pancreatic cancer cells PANO2 (**Figure 6P-S**).

Flow cytometric analysis further demonstrated that knockdown of UBE2W promoted apoptosis in MIA-Paca-2 and CFPAC-1 cells (**Figure 6K**, **6L** and **6M**, **6N**). Collectively, these results indicate that knockdown of UBE2W inhibits proliferation and promotes apoptosis in PC cells both in vitro and in vivo.

UBE2W promotes PC migration in vitro

Furthermore, we examined the migratory and metastatic potential of PC cells with differential UBE2W expression. Transwell invasion assays (**Figure 7A-H**) demonstrated that knockdown of UBE2W suppressed the invasive capacity of PC cells, whereas overexpression of UBE2W markedly promoted invasion. Similarly, wound healing assays (**Figure 7I-P**) showed that knockdown of UBE2W impaired the migratory capacity of PC cells, whereas overexpression of UBE2W significantly enhanced migration.

p53 is a interacting protein of UBE2W

To investigate the mechanisms by which UBE2W regulates PC progression, we conducted gene set enrichment analysis (GSEA). The results revealed that UBE2W was positively associated with pathways including the UV-induced stress response, protein secretion, and androgen response, while showing negative associations with oxidative phosphorylation, DNA damage repair, and the p53 signaling pathway (**Figure 8A**).

To further elucidate the molecular mechanism through which UBE2W promotes tumorigenesis in pancreatic cancer, we employed proteomics combined with co-immunoprecipitation and mass spectrometry (Co-IP/MS) to identify UBE2W-specific substrate proteins. Total proteins were extracted from HEK293T cells overexpressing UBE2W for Co-IP pull-down assays. Differential protein bands identified by Western blotting were subjected to mass spectrometry, revealing 959 candidate proteins. Repeating the experiment using entire gel lanes from the control and experimental groups revealed 374 downregulated and 414 upregulated proteins. Intersection analysis of the two datasets identi-

Table 2. Univariate and multivariate Cox proportional-hazards regression analyses for patients with PC

Variables	Univariate analysis			Multivariate analysis		
	HR	95% CI	P	HR	95% CI	P
Sex						
Female	reference			reference		
Male	0.786	0.511-1.208	0.356			
Age (yr)						
< 60	reference			reference		
≥ 60	1.188	0.794-1.778	0.482			
Tumor size (cm)						
< 4	reference			reference		
≥ 4	1.069	0.712-1.606	0.786			
Differentiation status						
Poor differentiation	reference			reference		
Moderate differentiation	0.645	0.387-1.075	0.157			
Well differentiation	0.435	0.217-0.869	0.048			
Vascular invasion status						
No	reference			reference		
Yes	1.179	0.783-1.775	0.506			
Neural tract invasion status						
No	reference			reference		
Yes	1.312	0.861-1.998	0.288			
CEA						
< 4.7	reference			reference		
≥ 4.7	0.869	0.546-1.382	0.619			
CA125						
< 35	reference			reference		
≥ 35	1.032	0.660-1.615	0.907			
CA199 (U/ml)						
< 27	reference			reference		
≥ 27	1.982	1.118-3.513	0.049	1.724	0.950-3.127	0.132
AFP (ng/ml)						
< 7	reference			reference		
≥ 7	0.879	0.472-1.635	0.732			
T stage						
T1+2	reference			reference		
T3+4	0.989	0.656-1.490	0.963			
N stage						
N0	reference			reference		
N1	1.420	0.904-2.229	0.201			
N2	1.502	0.727-3.100	0.356			
M stage						
M0	reference			reference		
M1	1.258	0.714-2.216	0.504			
Positive lymph nodes						
No	reference			reference		
Yes	1.736	1.143-2.637	0.030	1.391	0.896-2.158	0.217
UBE2W						
Low expression	reference			reference		
High expression	1.860	1.205-2.871	0.018	1.729	1.112-2.688	0.041

Note: T stage: Primary Tumor Stage; N stage: Regional Lymph Node Stage; M stage: Distant Metastasis Stage; CA199: Cancer Antigen 199; CA125: Cancer Antigen 125; CEA: Carcinoembryonic Antigen; AFP: Alpha-Fetoprotein.

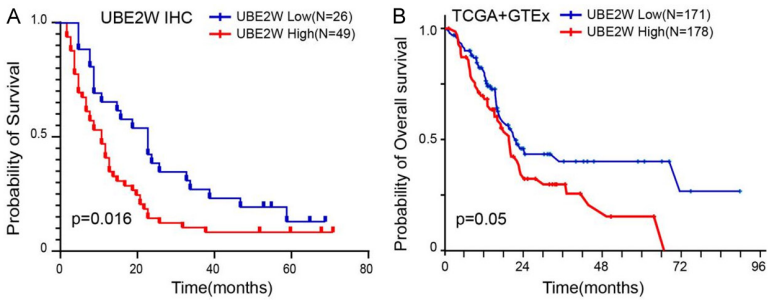

Figure 5. Poor prognosis in pancreatic cancer patients with high UBE2W expression. (A) The overall survival curves of 75 pancreatic cancer patients with high and low UBE2W expression were analyzed based on the immunohistochemical results, which is consistent with the expression trend in the TCGA database (B).

fied 33 downregulated and 28 upregulated proteins (**Figure 8B** and **8C**).

Co-IP validation of the 61 differentially expressed proteins confirmed a interaction between UBE2W and p53 (**Figure 8D**, **8E**). Similar results were observed in pancreatic cancer cell lines MIA-Paca-2 and CFPAC-1.

UBE2W regulates p53 subcellular distribution via K63-linked ubiquitination

Previous studies have demonstrated that p53 undergoes ubiquitination. Given that UBE2W functions as an E2 ubiquitin-conjugating enzyme, we investigated whether its interaction with p53 mediates ubiquitin modification. Overexpression of UBE2W enhanced p53 ubiquitination in HEK293T cells, a phenomenon that was also observed in MIA-Paca-2 cells (**Figure 9A** and **9B**). To elucidate the specific ubiquitin linkage type (K48 versus K63) mediated by UBE2W, we focused on the two predominant polyubiquitin chains: K48-linked chains, which primarily target proteins for proteasomal degradation, and K63-linked chains, which mainly regulate the functional modulation of target proteins.

We further investigated the specific ubiquitin linkage type underlying UBE2W-mediated p53 modification. HEK293T cells were co-transfected with HA-tagged UBE2W and ubiquitin mutants restricted to either K48 or K63 linkages. In vivo ubiquitination assays demonstrated that UBE2W specifically promotes K63-linked ubiquitination of p53 (**Figure 9C**). Notably, K63-ubiquitinated p53 was not degraded, as p53 protein levels remained stable in HEK293T cells even with increasing amounts of UBE2W plasmid (**Figure 9D**). These findings indicate that UBE2W catalyzes K63-linked ubiquitination of p53, conferring non-proteolyticregulatoryfunctions.

To validate the spatial regulatory role of K63-linked ubiquitination, nuclear-cytoplasmic fractionation was performed in UBE2W-overexpressing HEK293T cells. UBE2W-mediated K63 ubiquitination promoted the nuclear accumulation of p53 (**Figure 9E**). Collectively, these findings demonstrate that UBE2W regulates the p53 pathway by enhancing both its K63-linked ubiquitination and nuclear translocation.

UBE2W facilitates p53-mediated DNA damage repair and modulates apoptosis

HEK293T cells were co-transfected with p53-Flag and UBE2W-GFP plasmids, followed by VP16 treatment to induce DNA damage. Protein lysates were harvested at designated time points for the analysis of DNA repair and apoptosis-related markers. γH2AX, a well-established marker of DNA damage, displayed variable expression across treatment groups and time points. Compared with the control group (ct), transfection with p53-Flag significantly decreased γH2AX levels at 4 and 12 hours post-treatment. Notably, γH2AX levels at 12 hours were higher than at 4 hours, suggesting that p53 overexpression enhances DNA damage repair capacity. Transfection with UBE2W-GFP, either alone or in combination with p53-Flag, displayed similar trends, with the most pronounced DNA damage repair response observed in the p53-Flag + UBE2W-GFP co-transfection group (**Figure 10A**). These findings indicate a synergistic role of p53 and UBE2W in facilitating DNA damage repair.

Furthermore, knockdown of UBE2W activated apoptotic pathways, whereas overexpression of UBE2W inhibited apoptosis, as reflected by the differential expression of apoptosis-related proteins (**Figure 10B** and **10C**).

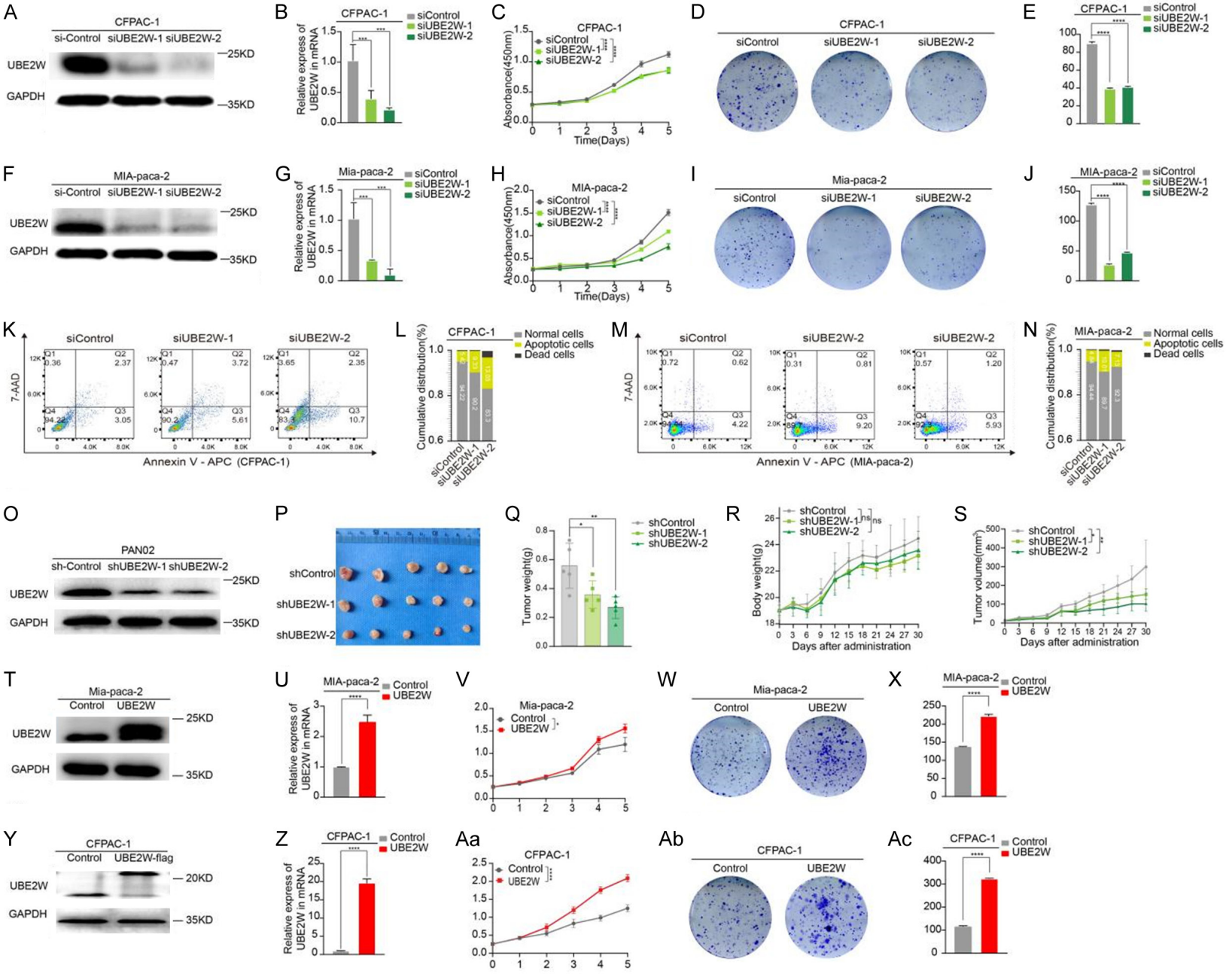
A
CFPAC-1
si-Control siUBE2W-1 siUBE2W-2
UBE2W
GAPDH
25KD
35KD
B
CFPAC-1
siControl
siUBE2W-1
siUBE2W-2
Relative express of UBE2W in mRNA
C
CFPAC-1
Absorbance(450nm)
Time(Days)
D
CFPAC-1
siControl
siUBE2W-1
siUBE2W-2
E
CFPAC-1
F
MIA-paca-2
G
Mia-paca-2
H
MIA-paca-2
I
Mia-paca-2
J
MIA-paca-2
K
siControl
siUBE2W-1
siUBE2W-2
7-AAD
Annexin V - APC (CFPAC-1)
L
CFPAC-1
Normal cells
Apoptotic cells
Dead cells
Cumulative distribution(%)
M
Annexin V - APC (MIA-paca-2)
N
MIA-paca-2
O
PAN02
sh-Control shUBE2W-1 shUBE2W-2
P
shControl
shUBE2W-1
shUBE2W-2
Q
Tumor weight(g)
R
Body weight(g)
Days after administration
S
Tumor volume(mm³)
T
Mia-paca-2
Control UBE2W
U
MIA-paca-2
V
Mia-paca-2
W
Mia-paca-2
X
MIA-paca-2
Y
CFPAC-1
Control UBE2W-flag
20KD
Z
CFPAC-1
Aa
CFPAC-1
Ab
CFPAC-1
Ac
CFPAC-1

Figure 6. UBE2W promotes the proliferation of pancreatic cancer and inhibits apoptosis. The knockdown and overexpression of UBE2W in PC cells were determined by western blotting (A, F, O, T, Y) and qRT-PCR (B, G, U, Z); (C, H, V, Aa; D, I, W, Ab) Cell proliferation was detected by CCK8 assay and Colony Formation, with quantitative analysis shown in (E, J, X, Ac); (K, M) Flow Cytometric Apoptosis Assay was used to detect the influence of UBE2W on cell apoptosis, with quantitative analysis of apoptotic cells shown in (L, N); (P-S) The subcutaneous tumorigenesis experiment in mice confirmed the effect of UBE2W on the proliferation of PC cells in vivo. Data are presented as the mean ± SD of at least three independent experiments. Statistical significance was determined as *P < 0.05, **P < 0.01, and ***P < 0.001.

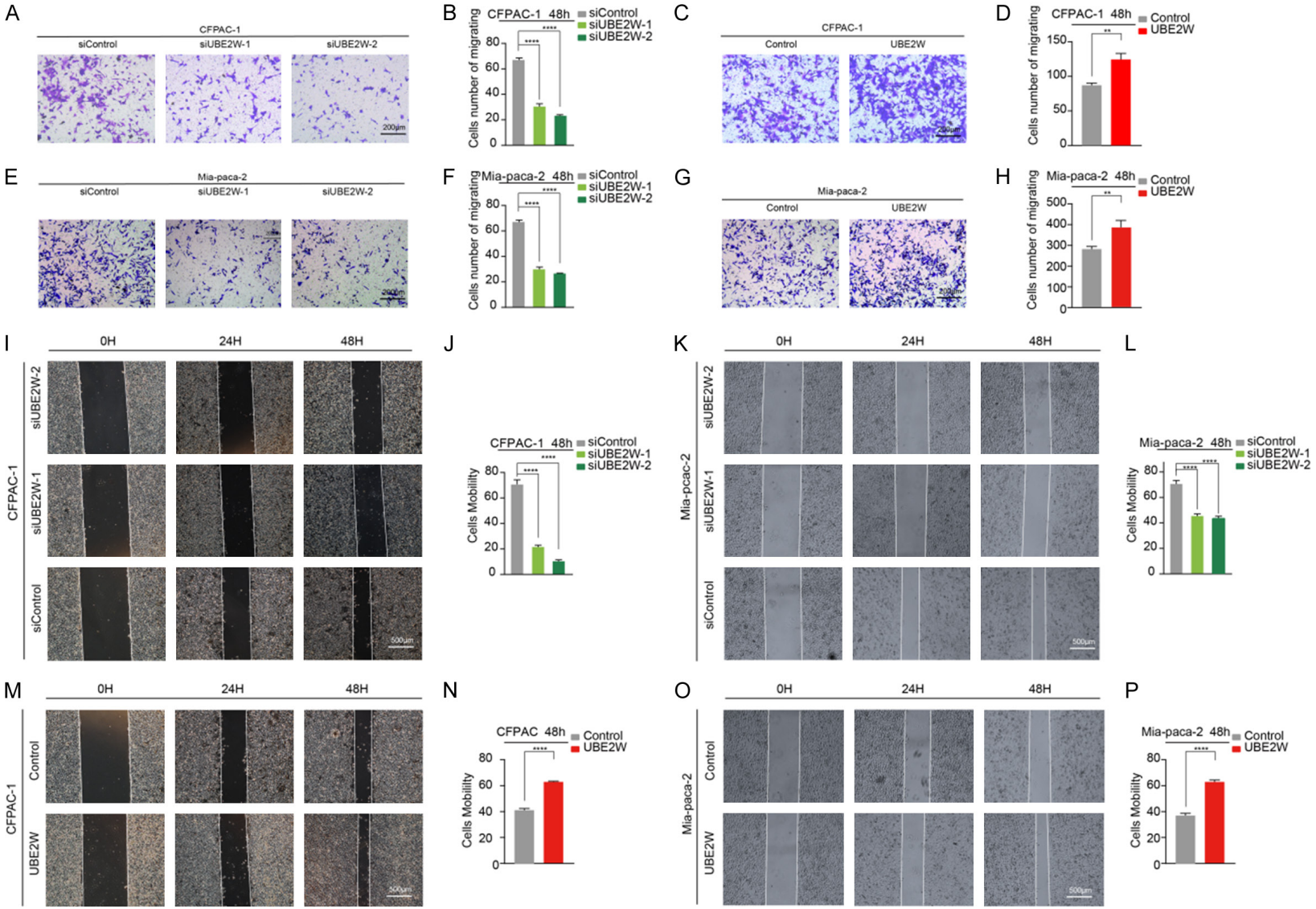

Figure 7. UBE2W promotes the migration and invasion of pancreatic cancer. (A, C, E, G) Wound healing assay was used to detect cell migration, with quantitative analysis of wound closure rates shown in (B, D, F, H); (I, K, M, O) Transwell assay was used to detect cell invasion, with quantitative analysis of invasive cell numbers shown in (J, L, N, P). Data are presented as the mean ± SD of at least three independent experiments. Statistical significance was determined as *P < 0.05, **P < 0.01, and ***P < 0.001.

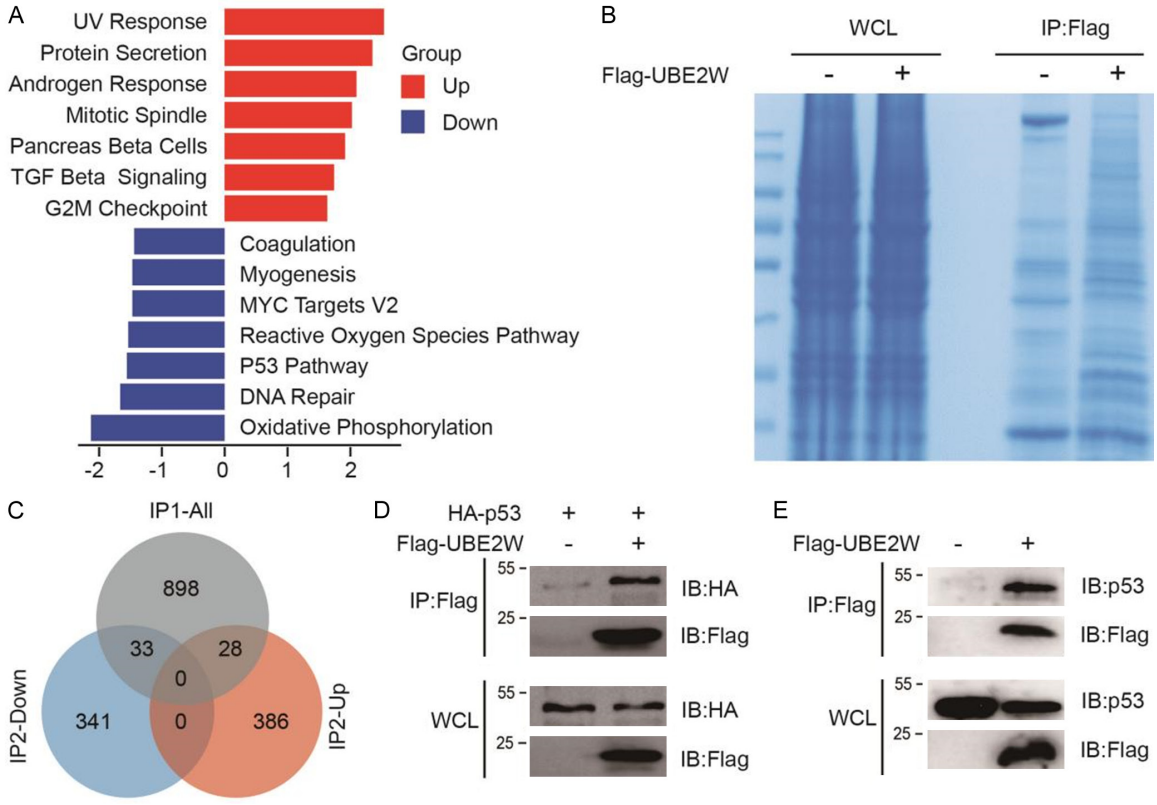

Figure 8. UBE2W interacts with P53. A. Single-gene GSEA pathway enrichment analysis of UBE2W; B. 293T cells overexpressing UBE2W were harvested and subjected to immunoprecipitation assay, followed by Coomassie Brilliant Blue staining; C. A Venn diagram shows the number of differential proteins identified in response to high UBE2W expression; D, E. HEK293 cells were co-transfected with Flag-UBE2W and HA-P53 plasmids for 48 h, then treated with MG132 (20 μM) for 4 h. Cell lysates were immunoprecipitated with a Flag-tag antibody, followed by western blot analysis using an HA-tag antibody or a p53 antibody.

Discussion

The global incidence of pancreatic cancer has continued to rise, and despite improvements in surgical techniques and systemic therapies, the number of new cases has nearly doubled over the past three decades. Substantial geographic disparities persist in the global distribution of pancreatic cancer, with developed regions exhibiting markedly higher incidence rates than developing areas. Western Europe reports the highest incidence (8.6 per 100,000), whereas South-Central Asia has the lowest (1.2 per 100,000). In 2020, the mortality rate reached 4.5 per 100,000, placing pancreatic cancer ninth among all cancer-related causes of death and seventh in total mortality-a ranking that has steadily increased over the past eight years [16].

Surgical management remains limited by the fact that most patients present with advanced-stage disease, at which point curative resection is no longer feasible [17]. As a result, pharmacologic therapies have become increasingly central to current treatment algorithms. Contemporary approaches-including multi-agent systemic chemotherapy, neoadjuvant chemoradiotherapy, genomic profiling-guided targeted therapies, and immune checkpoint blockade-are being actively investigated to improve therapeutic efficacy.

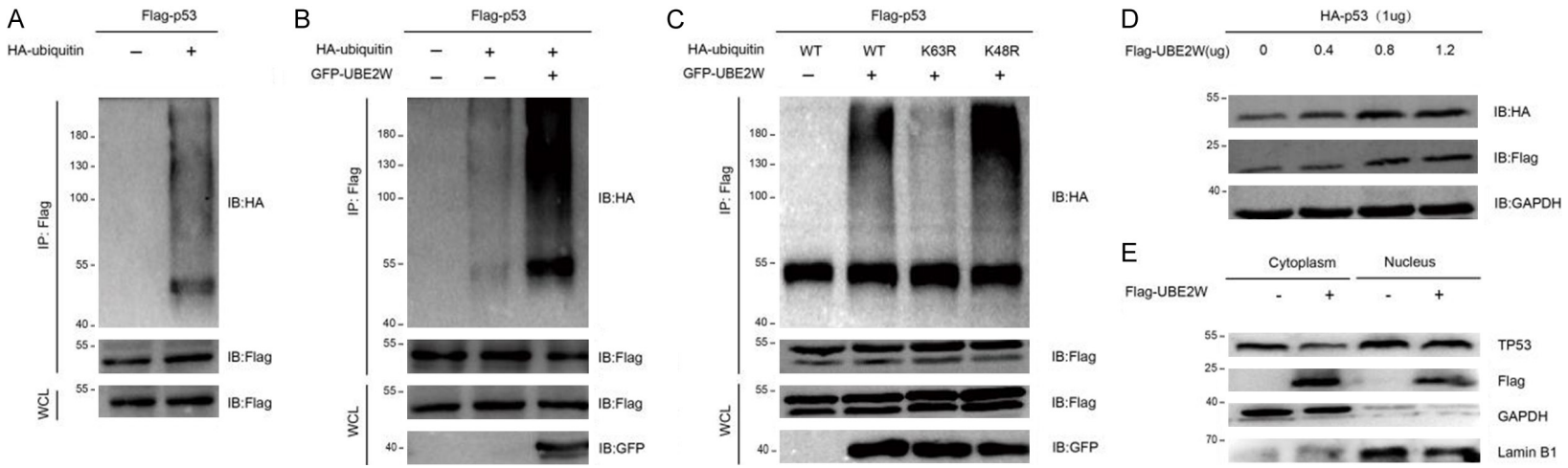

Figure 9. UBE2W regulates the intracellular distribution of P53 protein by inducing K63-linked ubiquitination. A. MIA-Paca-2 cells were co-transfected with HA-ubiquitin and Flag-p53 plasmids. Cell lysates were immunoprecipitated with the Flag-tag antibody, followed by western blot analysis using anti-Flag and anti-HA antibodies; B. MIA-Paca-2 cells were co-transfected with HA-ubiquitin, GFP-UBE2W, and Flag-p53 plasmids. Cell lysates were immunoprecipitated with the Flag-tag antibody, followed by western blot analysis using anti-Flag, anti-GFP, and anti-HA antibodies; C. MIA-Paca-2 cells were co-transfected with HA-ubiquitin, Flag-Ub-K48R, Flag-Ub-K63R, GFP-UBE2W, and Flag-p53 plasmids. Cell lysates were immunoprecipitated with the Flag-tag antibody, followed by western blot analysis using anti-Flag, anti-GFP, and anti-HA antibodies; D. MIA-Paca-2 cells were transiently co-transfected with HA-p53 plasmid and different doses of Flag-UBE2W. Cell lysates were immunoprecipitated with the Flag-tag antibody, followed by western blot analysis using anti-Flag, anti-GAPDH, and anti-HA antibodies; E. MIA-Paca-2 cells were transiently transfected with Flag-UBE2W, and cytoplasmic and nuclear proteins were extracted separately for western blot analysis using an anti-p53 antibody.

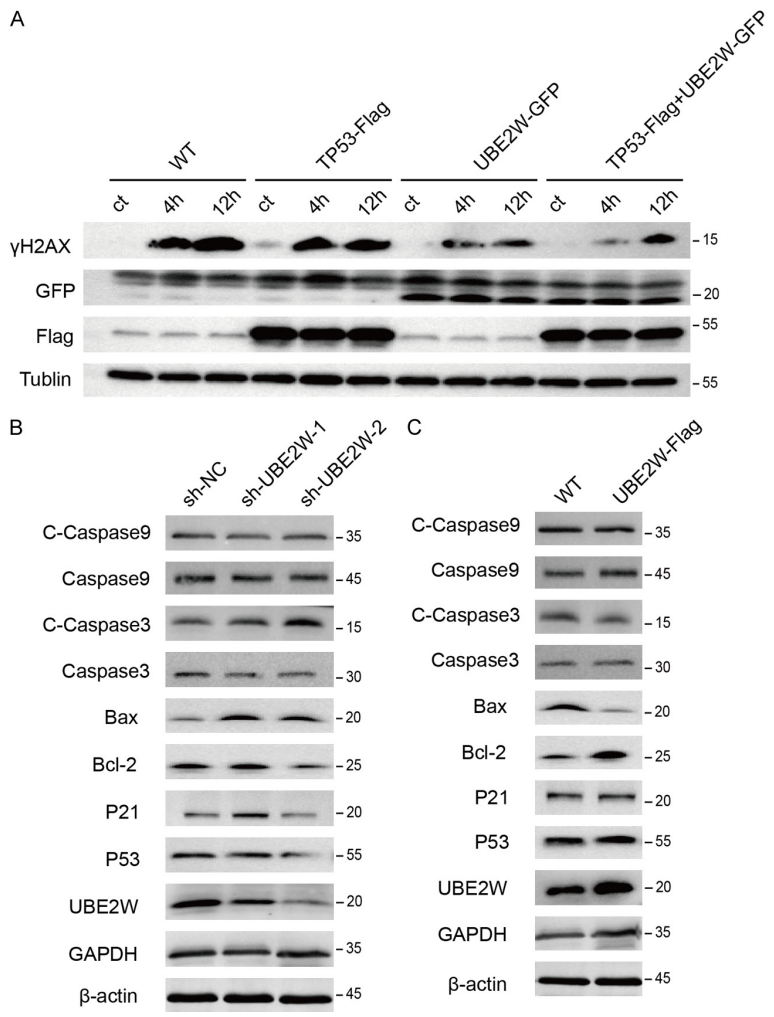

Figure 10. UBE2W and p53 exhibit a synergistic role in promoting DNA damage repair and inhibit apoptotic pathways in pancreatic cancer cells. A. MIA-Paca-2 cells were transfected individually or co-transfected with HA-ubiquitin, GFP-UBE2W, and Flag-p53 plasmids. After 24 hours, proteins were extracted at 0 h, 4 h, and 12 h following VP16 treatment, and western blot analysis was performed using an anti-γH2AX antibody; B, C. MIA-Paca-2 cells were transfected with sh-UBE2W and Flag-UBE2W, and western blot analysis was conducted using an anti-UBE2W antibody, anti-p53 antibody, and antibodies related to the apoptotic pathway.

Future research should prioritize the development of targeted therapeutics and immune checkpoint modulators suitable for prospective clinical evaluation, with the goal of enhancing the clinical benefit of first-line systemic chemotherapy. Emerging evidence from early studies [18, 19] underscores the potential of this strategic shift, highlighting targeted agents and immunotherapeutic approaches as promising avenues for advancing pancreatic cancer management.

Recent studies have increasingly shown that members of the ubiquitin-conjugating enzyme (E2) family exert critical regulatory functions in tumor initiation and progression [20-22]. For example, Jiang et al. [23] demonstrated that UBE2T facilitates RING1-mediated ubiquitination of p53, thereby relieving p53-dependent transcriptional repression of ribonucleotide reductase subunits M1 and M2 (RRM1/2). This derepression enhances pyrimidine biosynthesis and mitigates replication stress, ultimately promoting tumor cell proliferation. Their study further identified pentagalloylglucose (PGG) as a potent inhibitor of UBE2T and a sensitizer to gemcitabine. In addition, Cao et al. [24] demonstrated that UBE2C promotes pancreatic cancer progression and metastasis by interacting with EGFR and activating the PI3K-Akt signaling pathway. Moreover, UBE2C has been shown to regulate cell proliferation and epithelial-mesenchymal transition (EMT) during the development of pancreatic ductal adenocarcinoma (PDAC) [25]. Another study demonstrated that UBE2F deficiency suppresses the MAPK-c-Myc axis by inhibiting CRL5ASB11 E3 ligase-mediated ubiquitination of DIRAS2, highlighting the UBE2F-CRL5ASB11 axis as a potential therapeutic target in pancreatic cancer. Moreover, the expression levels of UBE2F or DIRAS2 may serve as prognostic biomarkers in PDAC [26]. Collectively, these findings underscore the critical roles of E2 enzymes in key pancreatic cancer processes, including cell proliferation, epithelial-mesenchymal transition (EMT), apoptosis, and chemoresistance.

Building on this evidence, our bioinformatics analysis identified BIRC6, UBE2Q2, and UBE2W as differentially expressed E2 family members in pancreatic tumors compared with adjacent normal tissues, exhibiting pro-metastatic functions and conferring resistance to commonly

used chemotherapeutics, including 5-FU, paclitaxel, and oxaliplatin. Further data mining revealed that UBE2W is markedly overexpressed in pancreatic cancer, showing a strong correlation with chemoresistance and poor clinical prognosis. Elucidating the biological functions of UBE2W and the molecular mechanisms underlying therapeutic resistance and aggressive tumor phenotypes may reveal novel diagnostic biomarkers and guide the development of targeted small-molecule inhibitors for pancreatic cancer.

UBE2W, a Class I ubiquitin-conjugating enzyme consisting solely of a ubiquitin-conjugating (UBC) domain, is overexpressed in 23 malignancies across pan-cancer analyses, including pancreatic adenocarcinoma (PAAD), glioblastoma (GBM), and stomach adenocarcinoma (STAD). From a prognostic perspective, UBE2W shows significant associations with survival outcomes-including overall survival (OS), disease-specific survival (DSS), disease-free interval (DFI), and progression-free interval (PFI)-across nine cancer types, notably pancreatic adenocarcinoma (PAAD), kidney renal clear cell carcinoma (KIRC), and uveal melanoma (UVM). In particular, UBE2W is highly expressed in PAAD and is strongly correlated with poor survival outcomes.

Our clinical validation using human tissue specimens confirmed the overexpression of UBE2W in pancreatic cancer, with elevated UBE2W levels significantly associated with poor patient prognosis. Clinicopathological analyses further revealed that high UBE2W expression correlated with perineural invasion ($P = 0.024$), increased numbers of positive lymph nodes ($P = 0.042$), and elevated serum levels of CA19-9 ($P = 0.016$) and CA125 ($P = 0.045$).

Functional experiments demonstrated that UBE2W knockdown markedly inhibited pancreatic cancer cell proliferation, colony formation, migration, and invasion, whereas UBE2W overexpression enhanced these oncogenic phenotypes. Collectively, these findings establish UBE2W as a key driver of pancreatic cancer progression.

The tumor microenvironment (TME) in PC is closely linked to chemoresistance [27-29]. Notably, UBE2W has also been implicated in modulating responses to tumor immunotherapy. Yuan et al. [15] reported that UBE2W is aberrantly expressed in breast cancer, where its elevated expression promotes tumor immunosuppression, metastasis, and resistance to endocrine therapy, ultimately contributing to poor patient prognosis. These findings suggest that UBE2W may serve as a potential biomarker for both prognosis and tumor-infiltrating immune cells. Wang et al. [30] further reported that Ube2w knockout (KO) mice exhibited a 50% reduction in testicular and thymic organ weights, which correlated with high UBE2W expression in these tissues, highlighting its functional role in the immune and male reproductive systems. However, these studies did not investigate the relationships between UBE2W and other immune features.

To address this gap, we first examined the association between UBE2W expression and immune infiltration scores. UBE2W exhibited significant negative correlations with stromal and immune scores in five cancer types, suggesting that its overexpression may suppress patient immune responses and consequently impair the efficacy of immunotherapy. Additionally, UBE2W expression was significantly correlated with various immune cells-including B cells, $CD4^+$ T cells, $CD8^+$ T cells, neutrophils, macrophages, and dendritic cells (DCs)-across 38 tumor types. Targeting immune checkpoint genes has been shown to reverse the immunosuppressive TME and reactivate antitumor immunity [31, 32]. Intriguingly, UBE2W exhibited positive correlations with multiple immune checkpoint genes, including C10orf54, CD274 (PD-L1), HAVCR2 (TIM-3), and IL10. These findings suggest that UBE2W may contribute to tumor immune evasion and provide potential insights for the development of immune checkpoint inhibitors.

To elucidate the mechanism by which UBE2W exerts its oncogenic effects in pancreatic cancer, we further demonstrated that UBE2W physically interacts with the p53 protein. As one of the most pivotal tumor suppressors, p53 inhibits tumor progression by inducing cell cycle arrest, promoting apoptosis, and suppressing metastasis. The regulation of p53 activation, inactivation, and degradation is primarily mediated by post-translational modifications (PTMs) [33-35]. Among these, ubiquitination-a key PTM of p53-has been extensively studied [36-40]. For instance, studies have

reported that UBE2T-mediated p53 degradation promotes gemcitabine resistance in pancreatic cancer by enhancing pyrimidine biosynthesis and alleviating replication stress, suggesting that combining UBE2T-targeted agents with gemcitabine may improve patient survival [36]. Yuan Dong et al. [37] demonstrated that CLDN6 in colon cancer enhances p53 stability and inhibits colorectal cancer proliferation by modulating ubiquitination to facilitate nuclear translocation of the PTEN/AKT/MDM2 pathway. Additionally, studies on TRIM family proteins highlight their regulatory roles in p53 signaling: TRIM45 stabilizes p53 via K63-linked ubiquitination, thereby inhibiting glioma progression [38]; TRIM31 induces K63-linked ubiquitination of p53 through its RING domain while competitively blocking the MDM2-p53 interaction, preventing MDM2-mediated K48-linked ubiquitination and stabilizing p53 to suppress breast cancer [39]; and TRIM67 exerts antitumor effects by activating the p53 pathway, with the TRIM67/p53 axis representing a novel therapeutic target to enhance chemotherapy efficacy in colorectal cancers harboring wild-type p53 but exhibiting impaired p53 signaling [40].

In this study, UBE2W promotes K63-linked ubiquitination of p53, which does not induce proteasomal degradation but instead modulates the subcellular localization of ubiquitinated p53. We observed that ubiquitinated p53 predominantly accumulates in the nucleus, and cells co-transfected with TP53-Flag and UBE2W-GFP plasmids exhibited enhanced activation of nuclear DNA damage repair pathways. Further studies demonstrated that UBE2W regulates the subcellular localization of p53 through ubiquitination, thereby affecting DNA damage repair and apoptotic pathways to modulate pancreatic cancer cell behavior.

This study has several limitations that should be acknowledged. Although we propose that UBE2W promotes pancreatic cancer malignancy by mediating K63-linked ubiquitination of p53 and perturbing DNA damage repair and apoptotic pathways, the specific binding sites responsible for the UBE2W-p53 interaction remain undefined.

The identity of the E3 ubiquitin ligase that cooperates with UBE2W to modulate p53 remains unelucidated in the present study. Although our prior co-immunoprecipitation (co-IP) assays confirmed that UBE2W physically interacts with the TRIM21 protein in cellular contexts, no further experimental evidence was obtained to verify that TRIM21-functioning as an E3 ubiquitin ligase-synergizes with UBE2W to jointly regulate p53.

Published literature has demonstrated that the RING domain of TRIM21 catalyzes K48-linked polyubiquitination of mutant p53 (mutp53), leading to its degradation via the proteasomal pathway. In cell lines such as colorectal cancer HT29 and breast cancer SK-BR3 cells, TRIM21 overexpression markedly reduces mutp53 protein levels, whereas TRIM21 knockout results in the accumulation of mutp53 [41]. In pancreatic ductal adenocarcinoma (PDAC), mutant p53 or Kras can upregulate TRIM21 expression, which in turn induces the ubiquitination and degradation of TAp63α-a member of the p53 family [42]. The loss of TAp63α relieves the transcriptional repression of IL20RB, thereby activating the JAK1-STAT3 signaling pathway and promoting tumor metastasis and chemoresistance. Additionally, the RNA-binding protein HuR enhances TRIM21 translation by binding to the 3' untranslated region (3'UTR) of TRIM21 mRNA, while TRIM21 forms a negative feedback loop by degrading HuR, which modulates p53 protein synthesis in response to ultraviolet (UV) irradiation [43].

Building on existing literature and preliminary experimental explorations in this study, we can infer that TRIM21 collaborates with UBE2W to regulate p53 ubiquitination. However, this hypothesis necessitates rigorous and well-designed experimental validation in future research to confirm its scientific validity.

Additionally, the patient cohort was relatively small, particularly owing to the limited availability of fresh specimens for protein expression validation.

In future studies, we aim to further elucidate the precise mechanisms by which UBE2W regulates DNA damage repair and apoptosis in pancreatic cancer, thereby providing a solid theoretical foundation for the development of UBE2W-targeted small-molecule inhibitors.

In summary, UBE2W is a pan-cancer gene differentially expressed across multiple malignan-

cies, correlating with patient survival outcomes in various tumor types and representing a potential therapeutic and prognostic biomarker. Its significant correlations with immune cell infiltration and immune checkpoint genes underscore its potential as a target for tumor immunotherapy. Mechanistically, UBE2W undermines the tumor-suppressive functions of p53 by mediating K63-linked ubiquitination to alter its subcellular localization, thereby promoting pancreatic cancer initiation and progression. Targeting the UBE2W-p53 axis represents a novel therapeutic strategy, and the development of specific inhibitors holds promise for improving clinical outcomes in pancreatic cancer patients.

Acknowledgements

This project was supported by Gansu Provincial Science and Technology Program (23JRRA1008, 23JRRA0979); University Faculty Innovation Fund Program (2024B-025); and Cuiying Science and Technology Innovation Program (CY2023-QN-B01); and Gansu Clinical Medical Research Center Construction Project (21JR7RA433).

Written informed consent was obtained from all patients.

Disclosure of conflict of interest

The authors declare that the research was conducted in the absence of any commercial or financial relationships that could be construed as a potential conflict of interest.

Address correspondence to: You-Cheng Zhang and Yong Fan, Department of General Surgery, Lanzhou University Second Hospital, Lanzhou University Second Clinical Medical College, No. 82 Cuiying Men, Chengguan District, Lanzhou 730000, Gansu, China. E-mail: zhangychmd@126.com (YCZ); ery_fany@lzu.edu.cn (YF)

References

[1] GBD 2017 Pancreatic Cancer Collaborators. The global, regional, and national burden of pancreatic cancer and its attributable risk factors in 195 countries and territories, 1990-2017: a systematic analysis for the global burden of disease study 2017. Lancet Gastroenterol Hepatol 2019; 4: 934-947.

[2] Giannone F, Capretti G, Abu Hilal M, Boggi U, Campra D, Cappelli C, Casadei R, De Luca R, Falconi M, Giannotti G, Gianotti L, Girelli R, Gollini P, Ippolito D, Limerutti G, Maganuco L, Malagnino V, Malleo G, Morone M, Mosconi C, Mrakic F, Palumbo D, Salvia R, Sgroi S, Zerbi A and Balzano G. Resectability of pancreatic cancer is in the eye of the observer: a multicenter, blinded, prospective assessment of interobserver agreement on NCCN resectability status criteria. Ann Surg Open 2021; 2: e087.

[3] Zhou B, Zhang SR, Chen G and Chen P. Developments and challenges in neoadjuvant therapy for locally advanced pancreatic cancer. World J Gastroenterol 2023; 29: 5094-5103.

[4] Ozaka M, Nakachi K, Kobayashi S, Ohba A, Imaoka H, Terashima T, Ishii H, Mizusawa J, Katayama H, Kataoka T, Okusaka T, Ikeda M, Sasahira N, Miwa H, Mizukoshi E, Okano N, Mizuno N, Yamamoto T, Komatsu Y, Todaka A, Kamata K, Furukawa M, Fujimori N, Katanuma A, Takayama Y, Tsumura H, Fukuda H, Ueno M and Furuse J; Hepatobiliary and Pancreatic Oncology Group of Japan Clinical Oncology Group (JCOG). A randomised phase II study of modified FOLFIRINOX versus gemcitabine plus nab-paclitaxel for locally advanced pancreatic cancer (JCOG1407). Eur J Cancer 2023; 181: 135-144.

[5] Hank T, Klaiber U, Hinz U, Schütte D, Leonhardt CS, Bergmann F, Hackert T, Jäger D, Büchler MW and Strobel O. Oncological outcome of conversion surgery after preoperative chemotherapy for metastatic pancreatic cancer. Ann Surg 2023; 277: e1089-e1098.

[6] Liu Y, Su Z, Tavana O and Gu W. Understanding the complexity of p53 in a new era of tumor suppression. Cancer Cell 2024; 42: 946-967.

[7] Andrysik Z and Espinosa JM. Harnessing p53 for targeted cancer therapy: new advances and future directions. Transcription 2025; 16: 3-46.

[8] Huang Y, Che X, Wang PW and Qu X. p53/MDM2 signaling pathway in aging, senescence and tumorigenesis. Semin Cancer Biol 2024; 101: 44-57.

[9] Wang X, Yang J, Yang W, Sheng H, Jia B, Cheng P, Xu S, Hong X, Jiang C, Yang Y, Wu Z and Wang J. Multiple roles of p53 in cancer development: regulation of tumor microenvironment, m6A modification and diverse cell death mechanisms. J Adv Res 2025; 75: 539-560.

[10] Efe G, Rustgi AK and Prives C. p53 at the crossroads of tumor immunity. Nat Cancer 2024; 5: 983-995.

[11] Ge Y, Xiao B, Zhao R, Li B, Yang S, He KF, Gu HJ and Zuo S. CARMIL1 regulates liver cancer cell proliferation by activating the ERK/mTOR pathway through the TRIM27/p53 axis. Int Immunopharmacol 2024; 134: 112139.

[12] Lu X, Wang H and Yu T. TRIM6 promotes cell cycle and growth by modulating p53 signaling pathway in lung adenocarcinoma. Int J Gen Med 2025; 18: 2107-2117.
[13] Du X, Song H, Shen N, Hua R and Yang G. The molecular basis of ubiquitin-conjugating enzymes (E2s) as a potential target for cancer therapy. Int J Mol Sci 2025; 18: 2107-2117.
[14] Maure JF, Moser SC, Jaffray EG, F Alpi A and Hay RT. Loss of ubiquitin E2 Ube2w rescues hypersensitivity of Rnf4 mutant cells to DNA damage. Sci Rep 2016; 6: 26178.
[15] Yuan Y, Xiao WW, Xie WH, Li RZ and Gao YH. Prognostic value of ubiquitin E2 UBE2W and its correlation with tumor-infiltrating immune cells in breast cancer. BMC Cancer 2021; 21: 479.
[16] Luo W, Wang J, Chen H, Ye L, Qiu J, Liu Y, Wang R, Weng G, Liu T, Su D, Tao J, Ding C, You L and Zhang T. Epidemiology of pancreatic cancer: new version, new vision. Chin J Cancer Res 2023; 35: 438-450.
[17] Khorana AA, McKernin SE, Berlin J, Hong TS, Maitra A, Moravek C, Mumber M, Schulick R, Zeh HJ and Katz MHG. Potentially curable pancreatic adenocarcinoma: ASCO clinical practice guideline update. J Clin Oncol 2019; 37: 2082-2088.
[18] Zhang R, Li C, Zhang S, Kong L, Liu Z, Guo Y, Sun Y, Zhang C, Yong Y, Lv J, Lu M, Liu M, Wu D, Zhang T, Yang H, Wei D, Chen Z and Bian H. UBE2S promotes glycolysis in hepatocellular carcinoma by enhancing E3 enzyme-independent polyubiquitination of VHL. Clin Mol Hepatol 2024; 30: 771-792.
[19] Hilmi M, Delaye M, Muzzolini M, Nicolle R, Cros J, Hammel P, Cardot-Ruffino V and Neuzillet C. The immunological landscape in pancreatic ductal adenocarcinoma and overcoming resistance to immunotherapy. Lancet Gastroenterol Hepatol 2023; 8: 1129-1142.
[20] Qi S, Guan X, Zhang J, Yu D, Yu X, Li Q, Yin W, Cheng XD, Zhang W and Qin JJ. Targeting E2 ubiquitin-conjugating enzyme UbcH5c by small molecule inhibitor suppresses pancreatic cancer growth and metastasis. Mol Cancer 2022; 21: 70.
[21] Liu B, Liu R, Zhang X, Tian L, Li Z and Yu J. Ubiquitin-conjugating enzyme E2T confers chemoresistance of colorectal cancer by enhancing the signal propagation of Wnt/β-catenin pathway in an ERK-dependent manner. Chem Biol Interact 2025; 406: 111347.
[22] He X, Xiong S, Zhu Z, Sun J, Cao C and Wang H. Overexpression of ubiquitin-conjugating enzyme 2T induces radiotherapy resistance in hepatocellular carcinoma by enriching regulatory T cells in the tumor microenvironment. Nan Fang Yi Ke Da Xue Xue Bao 2024; 44: 1149-1158.
[23] Jiang X, Ma Y, Wang T, Zhou H, Wang K, Shi W, Qin L, Guan J, Li L, Long B, Wang J, Guan X, Ye H, Yang J, Yu Z and Jiao Z. Targeting UBE2T potentiates gemcitabine efficacy in pancreatic cancer by regulating pyrimidine metabolism and replication stress. Gastroenterology 2023; 164: 1232-1247.
[24] Cao JZ, Nie G, Hu H, Zhang X, Ni CM, Huang ZP, Qiao GL and Ouyang L. UBE2C promotes the progression of pancreatic cancer and glycolytic activity via EGFR stabilization-mediated PI3K-Akt pathway activation. J Gastrointest Oncol 2022; 13: 1444-1453.
[25] Wang X, Yin L, Yang L, Zheng Y, Liu S, Yang J, Cui H and Wang H. Silencing ubiquitin-conjugating enzyme 2C inhibits proliferation and epithelial-mesenchymal transition in pancreatic ductal adenocarcinoma. FEBS J 2019; 286: 4889-4909.
[26] Chang Y, Chen Q, Li H, Xu J, Tan M, Xiong X and Sun Y. The UBE2F-CRL5ASB11-DIRAS2 axis is an oncogene and tumor suppressor cascade in pancreatic cancer cells. Dev Cell 2024; 59: 1317-1332.e5.
[27] Sherman MH and Beatty GL. Tumor microenvironment in pancreatic cancer pathogenesis and therapeutic resistance. Annu Rev Pathol 2023; 18: 123-148.
[28] Hartupee C, Nagalo BM, Chabu CY, Tesfay MZ, Coleman-Barnett J, West JT and Moaven O. Pancreatic cancer tumor microenvironment is a major therapeutic barrier and target. Front Immunol 2024; 15: 1287459.
[29] Poyia F, Neophytou CM, Christodoulou MI and Papageorgis P. The role of tumor microenvironment in pancreatic cancer immunotherapy: current status and future perspectives. Int J Mol Sci 2024; 25: 9555.
[30] Wang B, Merillat SA, Vincent M, Huber AK, Basrur V, Mangelberger D, Zeng L, Elenitoba-Johnson K, Miller RA, Irani DN, Dlugosz AA, Schnell S, Scaglione KM and Paulson HL. Loss of the ubiquitin-conjugating enzyme UBE2W results in susceptibility to early postnatal lethality and defects in skin, immune, and male reproductive systems. J Biol Chem 2016; 291: 3030-3042.
[31] Khaliq AM, Rajamohan M, Saeed O, Mansouri K, Adil A, Zhang C, Turk A, Carstens JL, House M, Hayat S, Nagaraju GP, Pappas SG, Wang YA, Zyromski NJ, Opyrchal M, Lee KP, O'Hagan H, El Rayes B and Masood A. Spatial transcriptomic analysis of primary and metastatic pancreatic cancers highlights tumor microenvironmental heterogeneity. Nat Genet 2024; 56: 2455-2465.

[32] Yang C, Geng H, Yang X, Ji S, Liu Z, Feng H, Li Q, Zhang T, Zhang S, Ma X, Zhu C, Xu N, Xia Y, Li Y, Wang H, Yu C, Du S, Miao B, Xu L, Wang H, Cao Y, Li B, Zhu L, Tang X, Zhang H, Zhu C, Huang Z, Leng C, Hu H, Chen X, Yuan S, Jin G, Bernards R, Sun C, Zheng Q, Qin W, Gao Q and Wang C. Targeting the immune privilege of tumor-initiating cells to enhance cancer immunotherapy. Cancer Cell 2024; 42: 2064-2081.e19.

[33] Huang Y, Li W, Zhou Y, Bai J, Li N, Su Z and Cheng X. Strategies for p53 activation and targeted inhibitors of the p53-Mdm2/MdmX interaction. Cells 2025; 14: 583.

[34] Rusin M. The p53 protein - not only the guardian of the genome. Postepy Biochem 2024; 70: 71-87.

[35] Bakker MJ, Svensson O, So Rensen HV and Skepö M. Exploring the functional landscape of the p53 regulatory domain: the stabilizing role of post-translational modifications. J Chem Theory Comput 2024; 20: 5842-5853.

[36] Jiang X, Wang T, Zhao B, Sun H, Dong Y, Ma Y, Li Z, Wu Y, Wang K, Guan X, Long B, Qin L, Shi W, Shi L, He Q, Liu W, Li M, Xiao L, Zhou C, Sun H, Yang J, Guan J, Zhou H, Yu Z and Jiao Z. KRASG12D-driven pentose phosphate pathway remodeling imparts a targetable vulnerability synergizing with MRTX1133 for durable remissions in PDAC. Cell Rep Med 2025; 6: 101966.

[37] Dong Y, Xu W, Qi D, Qu H, Jin Q, Sun M, Wang X and Quan C. CLDN6 inhibits colorectal cancer proliferation dependent on restraining p53 ubiquitination via ZO-1/PTEN axis. Cell Signal 2023; 112: 110930.

[38] Zhang J, Zhang C, Cui J, Ou J, Han J, Qin Y, Zhi F and Wang RF. TRIM45 functions as a tumor suppressor in the brain via its E3 ligase activity by stabilizing p53 through K63-linked ubiquitination. Cell Death Dis 2017; 8: e2831.

[39] Guo Y, Li Q, Zhao G, Zhang J, Yuan H, Feng T, Ou D, Gu R, Li S, Li K and Lin P. Loss of TRIM31 promotes breast cancer progression through regulating K48- and K63-linked ubiquitination of p53. Cell Death Dis 2021; 12: 945.

[40] Wang S, Zhang Y, Huang J, Wong CC, Zhai J, Li C, Wei G, Zhao L, Wang G, Wei H, Zhao Z and Yu J. TRIM67 activates p53 to suppress colorectal cancer initiation and progression. Cancer Res 2019; 79: 4086-4098.

[41] Liu J, Zhang C, Xu D, Zhang T, Chang CY, Wang J, Liu J, Zhang L, Haffty BG, Zong WX, Hu W and Feng Z. The ubiquitin ligase TRIM21 regulates mutant p53 accumulation and gain of function in cancer. J Clin Invest 2023; 133: e164354.

[42] Li Z, Gao F, Liu X, Fan S, Qi Y, He M, Luo X, Nie X, Wang J, Wang Y, Xiao ZJ and Li C. The E3 ligase TRIM21 promotes progression of pancreatic ductal adenocarcinoma by down-regulating TAp63α and derepressing IL20RB. Sci Signal 2025; 18: eadv4579.

[43] Guha A, Nag S and Ray PS. Negative feedback regulation by HuR controls TRIM21 expression and function in response to UV radiation. Sci Rep 2020; 10: 11753.